

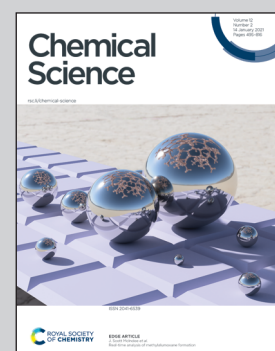


Showcasing research from Professor Tan Choon Hong's laboratory, Division of Chemistry and Biological Chemistry, School of Physical and Mathematical Sciences, Nanyang Technological University, 21 Nanyang Link, Singapore.

Enantioselective transition metal catalysis directed by chiral cations

Enantioselective transition metal catalysis directed by chiral cations is the amalgamation of chiral cation catalysis and organometallic catalysis. Thus far, three strategies have been revealed: ligand scaffold incorporated on chiral cation, chiral cation paired with transition metal 'ate'-type complexes, and ligand scaffold incorporated on achiral anion.

### As featured in:



See Xinyi Ye and Choon-Hong Tan, *Chem. Sci.*, 2021, **12**, 533.

**REVIEW**[View Article Online](#)  
[View Journal](#) | [View Issue](#)Cite this: *Chem. Sci.*, 2021, **12**, 533Received 18th October 2020  
Accepted 11th December 2020DOI: 10.1039/d0sc05734g  
[rsc.li/chemical-science](http://rsc.li/chemical-science)

## Enantioselective transition metal catalysis directed by chiral cations

Xinyi Ye<sup>\*a</sup> and Choon-Hong Tan<sup>\*b</sup>

Enantioselective transition metal catalysis directed by chiral cations is the amalgamation of chiral cation catalysis and organometallic catalysis. Thus far, three strategies have been revealed: ligand scaffolds incorporated on chiral cations, chiral cations paired with transition metal 'ate'-type complexes, and ligand scaffolds incorporated on achiral anions. Chiral cation ion-pair catalysis has been successfully applied to alkylation, cycloaddition, dihydroxylation, oxohydroxylation, sulfoxidation, epoxidation and C–H borylation. This development represents an effective approach to promote the cooperation between chiral cations and transition metals, increasing the versatility and capability of both these forms of catalysts. In this review, we present current examples of the three strategies and suggest possible inclusions for the future.

### 1. Introduction

In some chemical reactions, charged intermediates evolve and transform to neutral state target molecules. In order to overcome the energy barrier of such chemical reactions, using a suitable catalyst is the most straightforward and effective strategy. An ion-pair catalyst can be utilised to stabilise charged intermediates through ionic interactions, thereby allowing these reactions to proceed smoothly.<sup>1,2</sup> Chiral cations such as quaternary ammonium, guanidinium and quaternary phosphonium have been developed to control anionic intermediates<sup>2a</sup> while chiral anions such as borate and phosphate are utilised to control various cationic intermediates.<sup>2b</sup>

In chiral cation catalysis, the catalyst is paired with an anionic intermediate, usually an enolate resulting from proton abstraction of a reactant by an inorganic base. For example, reactions such as alkylation, Michael addition, Aldol reaction and Mannich reaction have enolate intermediates, and can be efficiently promoted using chiral cationic phase transfer catalysts.<sup>1b</sup> Other anions such as cyanide and fluoride can also be activated for cyanation and fluorination respectively using this approach. However, reactions involving reactants in a neutral electronic state or which are inert to inorganic bases cannot be catalysed using chiral cationic catalysts. Therefore, developing strategies to circumvent this weakness is eagerly anticipated in order to expand the scope of chiral cation catalysis. In order to activate allylic acetates for addition with glycinate Schiff base, Gong<sup>3a</sup> and Takemoto<sup>3b,c</sup> added palladium complexes in the

presence of chiral quaternary ammonium salts. Similar asymmetric allylations were also undertaken by Takemoto<sup>3d,e</sup> and Han<sup>3f</sup> using iridium complexes. While none of these reports have extensive mechanistic investigations, it was proposed that transition metals function to activate the electrophile in an independent catalytic cycle and work cooperatively with the chiral cation catalyst during the reaction pathway. The hypothesis since then is that if it is possible to allow organometallic catalysis to work synergistically through ion-pair interactions with chiral cations, new chemistry can be developed.<sup>2c,d</sup> Although this new approach is still in its infancy, three main categories have been identified; they are: (i) transition metal associated with a ligand scaffold incorporated on a chiral cation; (ii) chiral cation is paired with transition metal 'ate' complexes; and (iii) chiral cation paired with a transition metal, which is associated with an achiral anion containing a ligand scaffold (Fig. 1).

### 2. Strategy 1: ligand scaffold incorporated on a chiral cation

In 2014, Ooi and co-workers placed a phosphine on a side chain of a quaternary ammonium salt, allowing the cation to be an excellent ligand to Pd<sup>0</sup> (Scheme 1).<sup>4</sup> This novel cationic palladium complex achieved [3 + 2] cycloaddition between 5-vinyl-oxazolidinones and activated alkenes.<sup>4a</sup> A similar strategy was utilized in the addition of 5-vinylloxazolidinone to an imine.<sup>4b</sup> The authors hypothesised that the transition state consisted of a zwitterionic  $\pi$ -allylpalladium intermediate paired with quaternary ammonium (Scheme 1). Incorporation of a quaternary ammonium halide component allows both desirable halide–palladium contact and recognition of the anionic site through facile pairing with the chiral ammonium ion.

<sup>a</sup>College of Pharmaceutical Science & Collaborative Innovation Center of Yangtze River Delta Region Green Pharmaceuticals, Zhejiang University of Technology, 18 Chaowang Road, Hangzhou 310014, P. R. China. E-mail: xinyiye1020@zjut.edu.cn

<sup>b</sup>Division of Chemistry and Biological Chemistry, Nanyang Technological University, 21 Nanyang Link, Singapore 637371. E-mail: choonhong@ntu.edu.sg



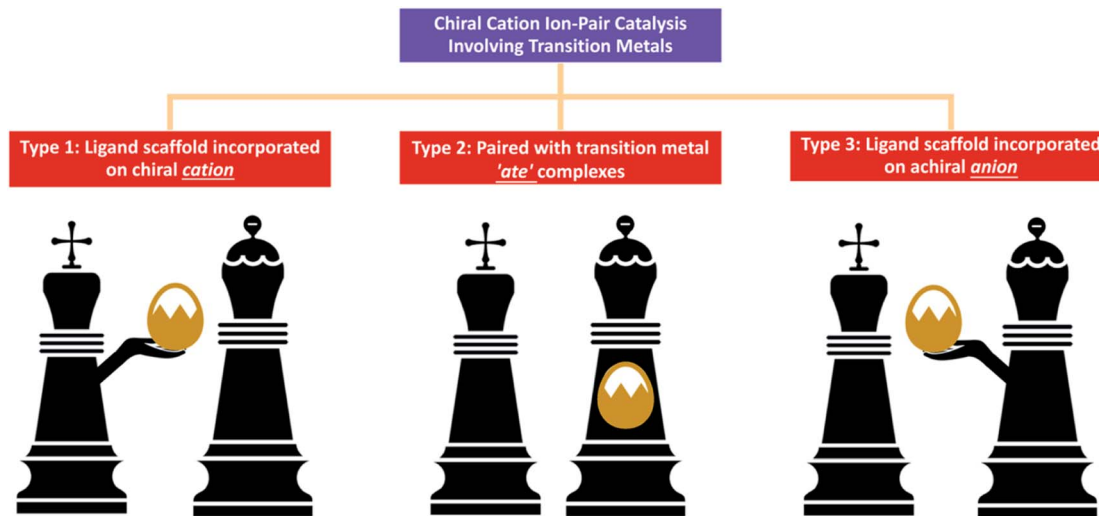
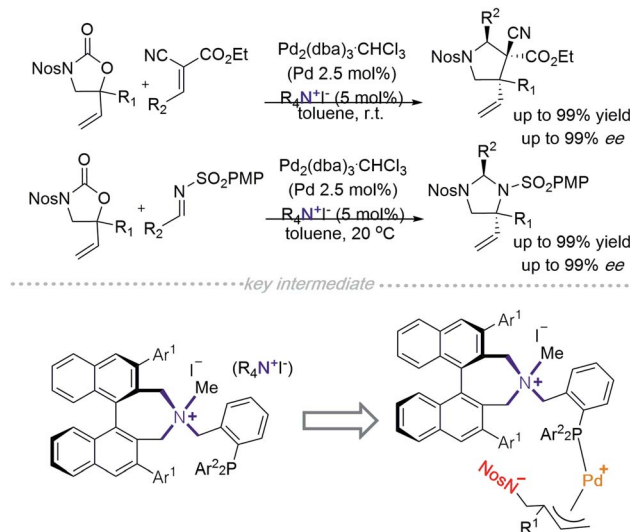


Fig. 1 Main strategies for incorporating organometallic complexes in chiral cationic ion-pair catalysis (king chess piece represents the chiral cation, queen chess piece represents the anion, and golden egg represents the metal complex).

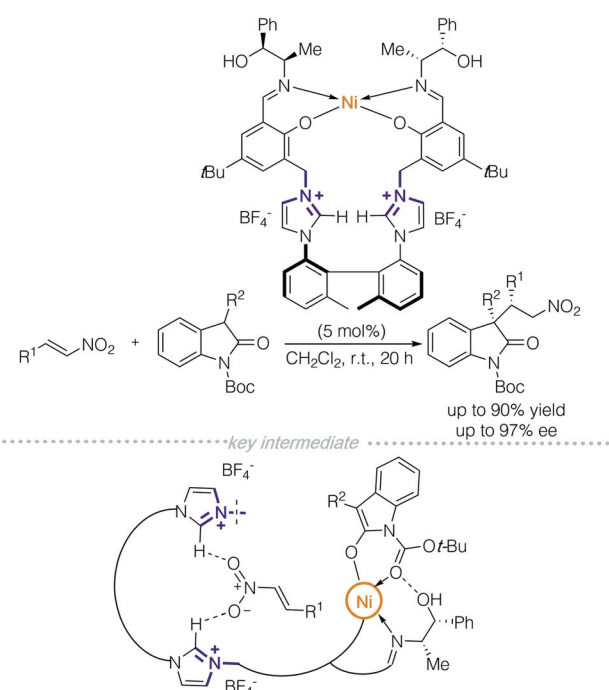


Scheme 1  $\text{Pd}^0$ /Phosphine scaffold incorporated quaternary ammonium-catalysed asymmetric  $[3 + 2]$  cycloaddition.

In 2015, the Peters group designed a multi-functional catalyst for diastereodivergent asymmetric 1,4-addition between oxindoles and nitroolefins (Scheme 2).<sup>5</sup> The polyfunctional catalyst consisted of a  $\text{Ni}^{II}$ -bis(polyoxyimine) motif with free hydroxyl groups and an axially chiral bis-imidazolium moiety as a chiral linker. Multiple non-covalent interactions were achieved through the bis-imidazolium cation, which provides electrostatic interactions, C–H hydrogen-bond donors and  $\pi$ -interactions. A  $\text{Ni}^{II}$ /Schiff-base complex functioned as a Lewis acid/Brønsted base and free hydroxyl groups allowed hydrogen-bonding. Each of the above factors (including the counterions) was evaluated by a series of control experiments. The authors proposed that the two reactants were controlled separately; one was activated by the chiral cation, and the other by the metallic

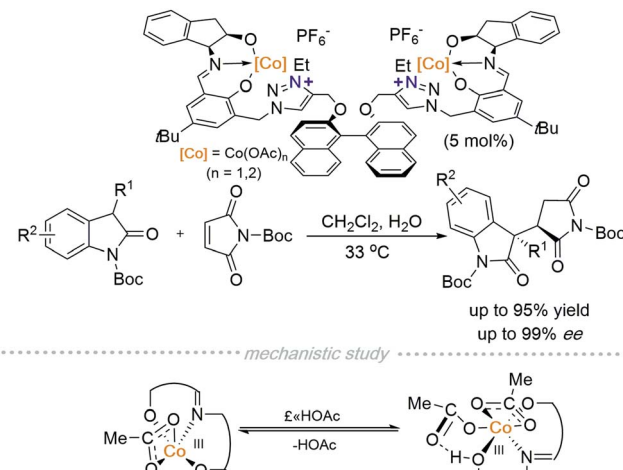
complex. At this moment, it is still unclear as to which non-covalent interaction is responsible for the stereochemical outcomes.

In 2019, Peters and co-workers reported another polyfunctional catalyst with two cobalt centres chelated in a tridentate manner to a Schiff base moiety that is connected to two triazolium cations and in turn linked *via* a chiral BINOL-based scaffold (Scheme 3).<sup>6</sup> A 1,4-addition reaction between 2-oxindoles and maleimides, catalysed by a  $\text{Co}^{III}$ /triazolium poly-functional catalyst can be conducted at room temperature. They



Scheme 2  $\text{Ni}^{II}$ /Schiff-base polyfunctional catalyst for an asymmetric 1,4-addition reaction.





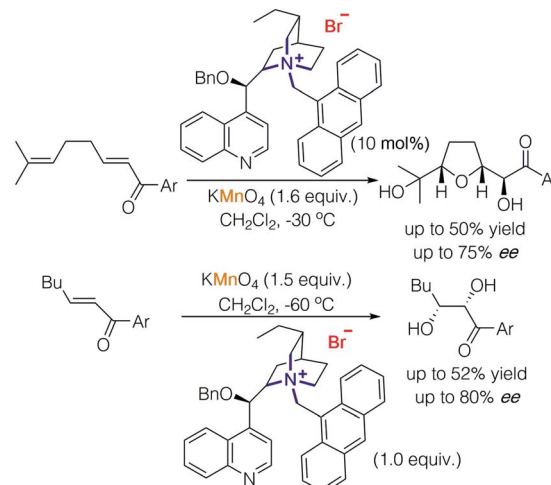
**Scheme 3**  $\text{Co}^{\text{III}}$ /Schiff-base polyfunctional catalyst for an asymmetric 1,4-addition reaction.

discovered that additives have a dramatic impact on reaction outcomes. For instance,  $\text{AcOH}$  provided the best results while  $\text{NaOAc}$  decreased the diastere- and enantioselectivity drastically. Although they were unable to elucidate the mechanism *via* single-crystal analysis of the catalytically active species, they observed the existence of one or two  $\text{AcOH}$  ligands on  $\text{Co}^{\text{III}}$  using ESI-MS. Probing further using DFT calculations suggests that equilibrium exists between monoacid coordinated  $\text{Co}^{\text{III}}$  and diacid coordinated  $\text{Co}^{\text{III}}$ . Evidence showed that a triplet spin state complex monoacid coordinated complex is more stable than a singlet diacid coordinated complex. Furthermore, the free coordination site on the paramagnetic monoacid coordinated  $\text{Co}^{\text{III}}$  allows binding of the pronucleophile suggesting that it is the catalytically active species. Recently, this group has also developed a new strategy for multi-functional cooperative Lewis acid/betaine (zwitterion) catalysis.<sup>7a,b</sup>

### 3. Strategy 2: chiral cations paired with transition metal 'ate' complexes

The rudiment of strategy 2 can be tracked back to the first report of alkaloid-catalysed oxidations,<sup>8,9</sup> in which stoichiometric permanganate worked as an oxidant but directed by a chiral cation to achieve enantioselectivity. In 2001, Brown and co-workers used cinchonidine-derived salts to promote oxidative cyclisation of 1,5-dienes using potassium permanganate, buffered with acetic acid (Scheme 4).<sup>8</sup> The reaction was proposed to proceed in a step-wise fashion consisting of dihydroxylation of dienes, oxidation by permanganate and condensation of diols. Through their study, they found that slightly acidic conditions led to an oxidative cyclisation reaction of 1,5-dienes and the formation of  $\alpha$ -ketols while slightly basic conditions promoted dihydroxylation.<sup>9</sup>

Basic conditions result in the decomposition of cinchonidine-derived chiral cations; hence, enantioselective dihydroxylation of enones was carried out with a stoichiometric amount of cinchonidine-derived chiral cations and

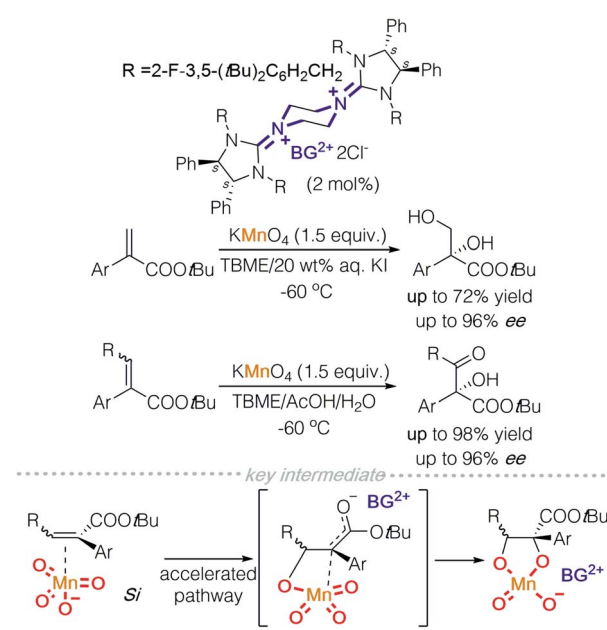


**Scheme 4** Cinchonidine-derived chiral cation paired with permanganate in asymmetric oxidative cyclisation and dihydroxylation.

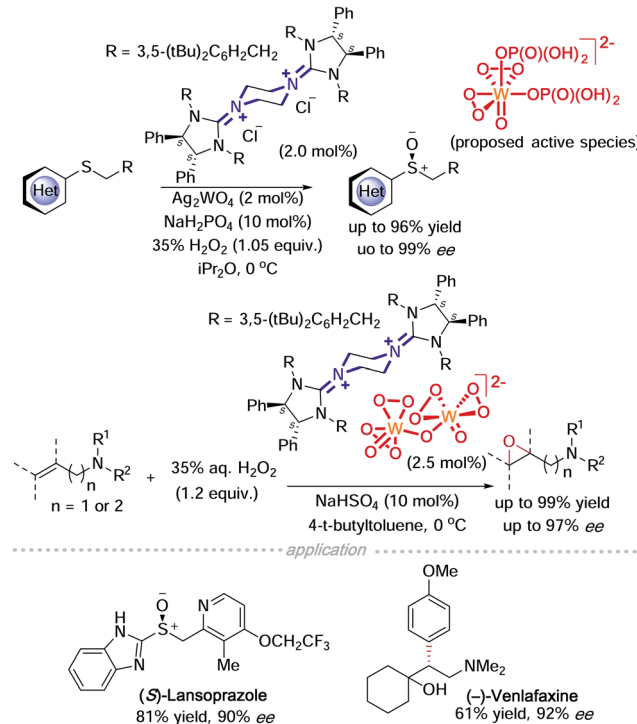
permanganate furnishing diols with good enantioselectivity (up to 80% ee).

In 2015, the Tan group demonstrated the use of permanganate for asymmetric oxidation in the presence of bisguanidinium (BG). Asymmetric dihydroxylation of  $\alpha$ -aryl acrylates and oxohydroxylation of trisubstituted enoates were achieved (Scheme 5).<sup>10</sup> The key intermediate was proposed to be a metallo-enolate formed as a result of permanganate insertion into an  $\alpha,\beta$ -unsaturated alkene. This mechanistic insight was deduced through observation of reaction by-products.

If a readily available external oxidant, such as hydrogen peroxide is present, it is then possible to use a catalytic amount of metal oxides. On this basis, Tan and co-workers took



**Scheme 5** Bisguanidinium permanganate in asymmetric dihydroxylation and oxohydroxylation.

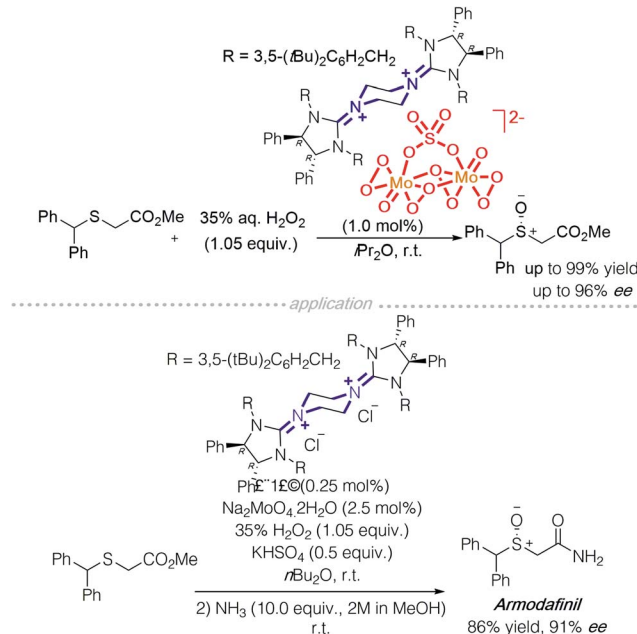


Scheme 6 Bisguanidinium heteropolytungstate in asymmetric sulfoxidation and epoxidation.

advantage of this possibility and used tungstate to catalyse asymmetric sulfoxidation of heterocyclic substituted thioethers and asymmetric epoxidation of allylic and homoallylic amides (Scheme 6).<sup>11a,b</sup> In a mechanistic study of the asymmetric sulfoxidation, the active counter ion was characterized using Raman spectroscopy and DFT calculations. A dihydrogen phosphate additive acts as a ligand coordinated to tungsten and DFT calculations indicate that a hydrogen bond exists between the two phosphate ligands. This strategy was successfully employed to synthesise (S)-lansoprazole.<sup>11a</sup> Homoallylic amides have been a difficult target for epoxidation. Tan and colleagues achieved a highly enantioselective asymmetric epoxidation on homoallylic amides using bisguanidinium tungstate. The active catalyst was isolated, characterised using single crystal X-ray diffraction and identified to be bisguanidinium tetraperoxotungstate,  $[BG]^{2+}$   $[W_2O_2(\mu-O)(O_2)]^{2-}$ . This strategy was successfully employed to synthesise (–)-venlafaxine.<sup>11b</sup>

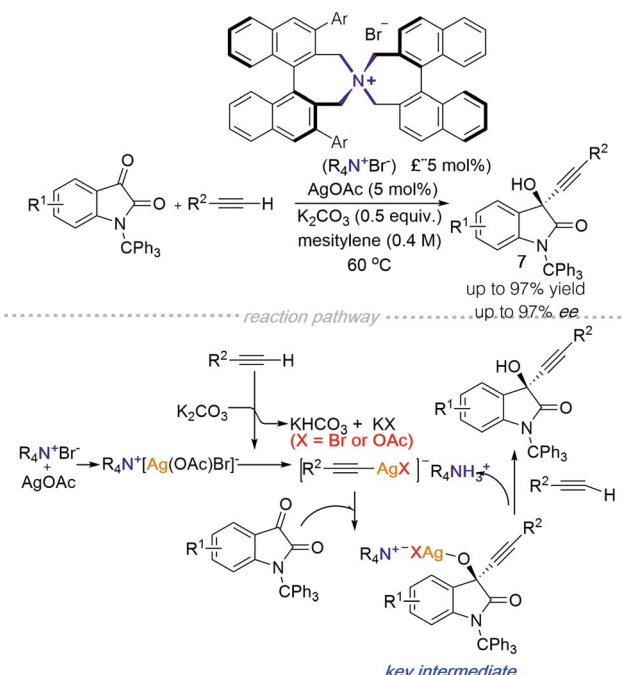
Another successful application of a transition metal ‘ate’-type counterion is heteropolytungstate. The active catalyst, bisguanidinium dinuclear oxodiperoxomolybdate  $[(\mu-SO_4)Mo_2O_2(\mu-O_2)_2(O_2)_2]^{2-}$ , was isolated and determined using single X-ray crystallography (Scheme 7). It proved effective in asymmetric sulfoxidation of electron-rich thioethers and successfully realised the synthesis of (R)-armodafinil on a gram-scale.<sup>12</sup>

In 2019, the Maruoka group reported an alkynylation of isatin derivatives catalysed using a chiral quaternary ammonium salt in the presence of silver acetate (Scheme 8).<sup>13</sup> A plausible mechanism of the reaction is described as follows: (1) the chiral quaternary ammonium salt interacts with silver acetate to generate  $Q^+[Ag(OAc)Br]^-$ ; (2) the terminal alkyne



Scheme 7 Bisguanidinium heteropolytungstate in asymmetric sulfoxidation.

deprotonated by  $K_2CO_3$  then associates with Ag, producing an alkynyl Ag-complex; (3) a substitution reaction between the alkynyl Ag-complex and isatin generates the key intermediate with high stereoselectivity; (4) finally, protonation by another alkyne molecule forms the final product and concomitantly regenerates the alkynyl Ag-ammonium ion pair.



Scheme 8  $C_2$ -symmetric quaternary ammonium argenteinate in asymmetric alkynylation.

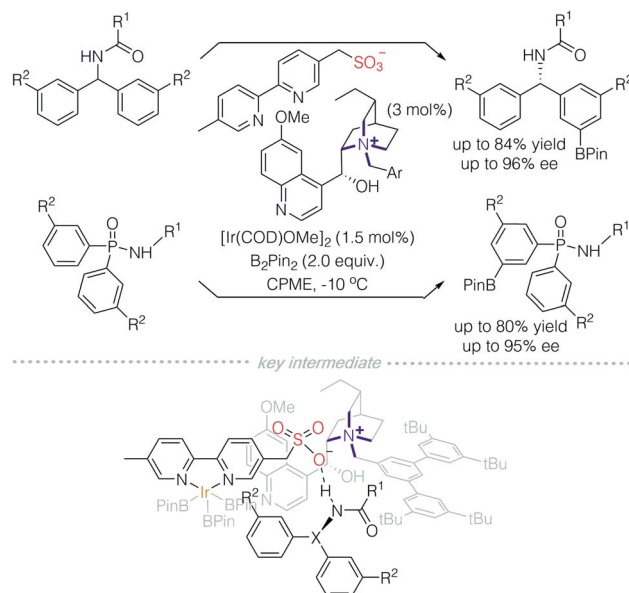


#### 4. Strategy 3: ligand scaffold incorporated on an achiral anion

In 2016, Phipps and co-workers developed a strategy for C–H functionalisation through the use of an anionic Ir-complex to control both cationic and neutral substrates (Scheme 9).<sup>14</sup> They demonstrated two modes of non-covalent interactions between substrates and the anionic Ir-complex. The first is quaternary ammonium containing benzylamine that is paired with a ligand possessing anionic sulfonate (model I).<sup>14a,c</sup> In the second approach, an amide protected benzylamine underwent hydrogen bonding with the sulfonate group on the ligand (model II).<sup>14b</sup> It should be noted that only model II falls under the scope of Strategy 3.

The essential characteristic of ion-pair catalysis is its catalytic efficiency due to effective interactions between its charged intermediates. Recently, Phipps and colleagues reported an enantioselective desymmetrisation through the use of an anionic Ir-complex, in conjunction with a chiral cationic catalyst (Scheme 10).<sup>15</sup> A quinine-derived chiral cation and sulfonyl modified bipyridine counterion were prepared as an ion pair catalyst. In the presence of iridium, borylation of an arene on benzhydrylamides and diaryl phosphinamides was achieved successfully. It was deduced that the counterion is an Ir-complex with a sulfonyl bipyridine ligand. The sulfonyl bipyridine ligand is both an ion pair to the chiral cation and site for hydrogen bonding with the acylamino group on the substrate. Consequently, remote C–H bond activation is achieved *via* the charge-inverted Ir-complex and enantioselectivity is induced by the quaternized alkaloid derivatives.

This methodology demonstrated excellent regioselectivity on aromatic rings. *Meta*-substitution is dominant even when R2 is on the *ortho*-position, despite a slight decrease in enantioselectivity. In comparison, when an uncharged bipyridine (dtbpy) was used, the regioslectivity was poor. This powerful methodology is also tolerant of a wide range of substituents on aromatic



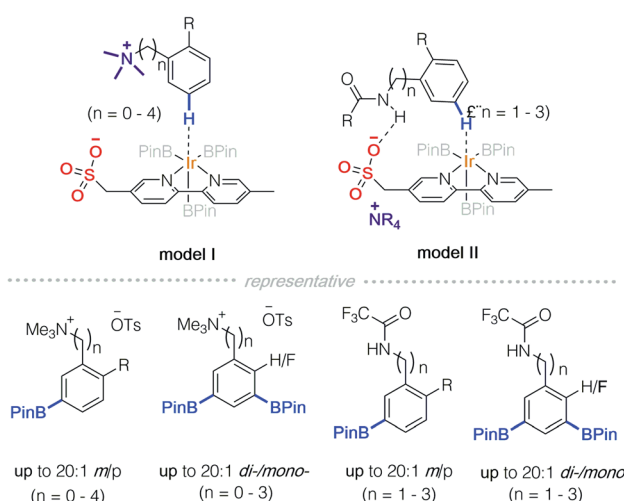
Scheme 10 Remote C–H activation catalysed by a quinine-derived chiral cation paired with an anionic Ir-complex.

rings, in particular, iodo-substituted arenes, which otherwise are incompatible with palladium catalysis.<sup>16</sup>

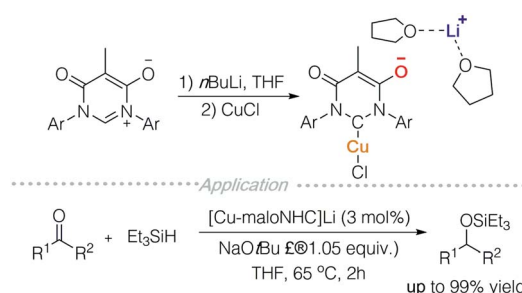
#### 5. Perspective

In accordance with the aforementioned strategies, several anionic transition metal complexes can be further developed for ion-pair catalysis. For instance, Lavigne and colleagues prepared an N-heterocyclic carbene decorated with a malonate backbone (*maloNHC*) (Scheme 11).<sup>17a</sup> It functions as an anionic ligand scaffold and can coordinate to metals such as rhodium,<sup>17b</sup> silver,<sup>17c</sup> iron,<sup>17a,d</sup> and copper. Metal-*maloNHC* was paired with Li(THF)<sub>2</sub><sup>+</sup> or quaternary ammonium and successfully used in skeletal rearrangement of enynes, hydrosilylation, hydroboration, and cyclopropanation. These reactions can potentially be carried out in an enantioselective manner with chiral quaternary ammonium salts.

Ion-pair transition metal complexes can be useful in electrochemistry and photochemistry. Lugan and co-workers prepared a  $\mu$ -vinylbis(carbene)-dimanganese complex (Scheme 12A), which is reduced to generate a radical anion and dianion

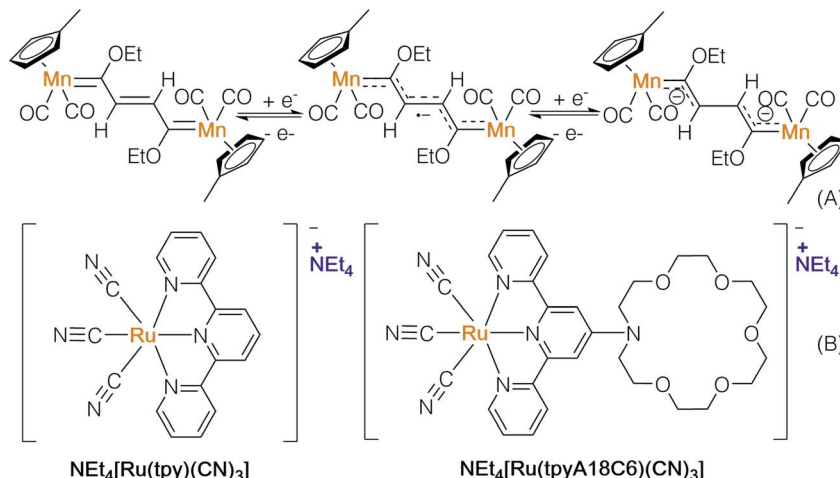


Scheme 9 Substrate interaction with a ligand scaffold incorporated on an achiral anion.



Scheme 11 Anionic NHC-complexed metal catalysis.



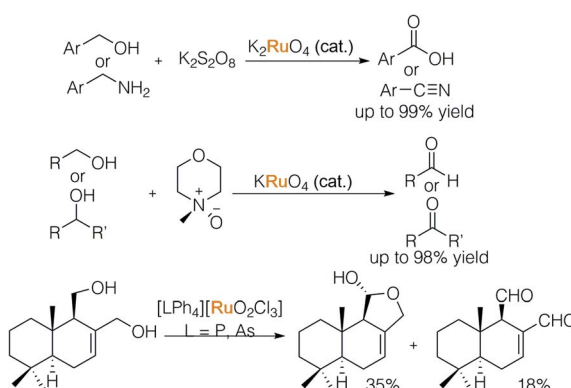


Scheme 12 Electron transfer processes of anionic metal complexes.

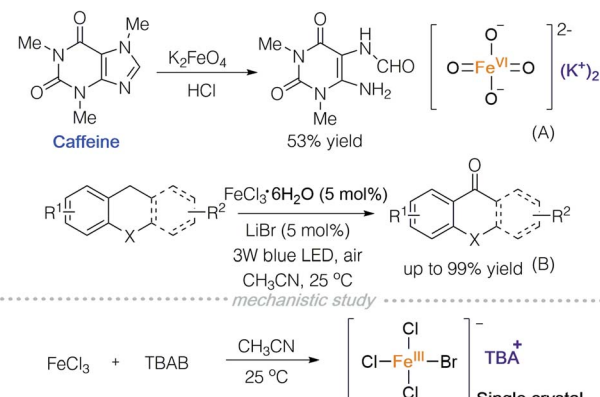
via cyclic voltammetry (CV).<sup>18</sup> The radical anion was characterized using EPR, showing a mixed-valence pattern of Mn<sup>0</sup>/Mn<sup>1</sup>, implying that the unpaired electron delocalized over two metal centres. The ability of the above-mentioned complexes to emit and absorb electrons may lead to potential application in electron transfer reactions.

The Yam group prepared a novel ruthenium anion complex  $\text{NEt}_4[\text{Ru}(\text{tpyA18C6})(\text{CN})_3]$  and used it as a mobile-phase additive to separate metal-ions in high-performance liquid chromatography (Scheme 12, B).<sup>19</sup> The solvatochromic behavior and photoluminescence of  $[\text{Ru}(\text{tpyA18C6})(\text{CN})_3]^-$  indicate its UV absorption properties. The solvent dependence of metal-to-ligand charge transfer (MLCT) absorption bands shows that active wavelengths are in the visible region. Through binding with a photosensitizer, the ion-pair ruthenium complex may serve as a catalyst in single electron transfer processes.

In 1979, Griffith and colleagues systematically studied ruthenate entities and their varied oxidative capacities (Scheme 13).<sup>20a</sup> In their initial report, a catalytic amount of ruthenate together with stoichiometric alkaline persulfate led to over-oxidation of an alcohol and amine to their corresponding acid and nitrile. The second oxidation step is inhibited by tuning the



Scheme 13 Tunable ruthenates in oxidation of alcohols and amines.



Scheme 14 Ferrate and iron 'ate'-type complexes in oxidations.

ruthenate and external oxidant. When per-ruthenate and *N*-methyl morpholine *N*-oxide (NMO) were used, primary and secondary alcohols were oxidized to aldehydes and ketones respectively.<sup>20b</sup> Subsequently, a new species  $[\text{LPh}_4]\text{RuO}_2\text{Cl}_3$  ( $\text{L} = \text{P, As}$ ) was found to be able to oxidise alcohols in the presence of alkenes.<sup>20c</sup> The tunable nature of Ru-complexes makes it possible to perform chemoselective oxidation.

Potassium ferrate is a common water purifying agent,<sup>21</sup> and can be used as an oxidant in organic synthesis. In 2017, Ray and co-workers used acid-activated potassium ferrate to oxidize caffeine (Scheme 14A).<sup>22</sup> Soon after, in 2018, Jiang and co-workers reported a photooxygenation of benzylic  $\text{sp}^3$  C-H using iron chloride and lithium bromide under visible light irradiation (Scheme 14B).<sup>23</sup> In order to study the active species in the reaction, they prepared TBA $[\text{FeCl}_3\text{Br}]$  and characterized it *via* single crystal X-ray diffraction (Scheme 14, mechanistic study).

## 6. Conclusion

The epitome of a chiral catalyst is one that it can be used for all enantioselective chemical reactions. This seems to be an



impossible dream as each reaction will have a different mode of activation. There lies a possibility of a universal chiral cation that can be paired with different anionic co-catalysts. The anion co-catalyst is responsible for promoting the reaction while the chiral cation provides the 'chiral space'. Inherently, optimisation of reactions will mainly involve the design of the non-chiral anionic co-catalyst instead of preparing a large number of chiral ligands as per current state-of-the-art approaches.

We have provided a synopsis of all major studies in chiral cation catalysis incorporating organometallic catalysis. We found that these new chemistries assimilated the advantages of both phase transfer and organometallic catalysis, leading to reduction of catalyst loading and expansion of scope of synthetic chemistry. We are confident that more developments in this area are forthcoming.

## Conflicts of interest

The authors declare no conflict of interest.

## Acknowledgements

We gratefully acknowledge the Zhejiang University of Technology (2020414801729), Nanyang Technological University (RG1/19 and RG2/20) and Ministry of Education Singapore (MOE2019-T2-1-091) for financial support.

## Notes and references

- 1 For selected reviews on asymmetric phase-transfer reactions see: (a) S. Shirakawa and K. Maruoka, *Angew. Chem., Int. Ed.*, 2013, **52**, 4312–4348; (b) T. Ooi and K. Maruoka, *Angew. Chem., Int. Ed.*, 2007, **46**, 4222–4266.
- 2 For selected reviews on asymmetric ion-pair catalysis see: (a) K. Bark and E. N. Jacobsen, *Angew. Chem., Int. Ed.*, 2013, **52**, 534–561; (b) M. Mahlau and B. List, *Angew. Chem., Int. Ed.*, 2013, **52**, 518–533; (c) L. Zong and C.-H. Tan, *Acc. Chem. Res.*, 2017, **50**, 842–856; (d) K. Ohmatsu and T. Ooi, *Top. Curr. Chem.*, 2019, **377**, 1–22.
- 3 (a) G. Chen, Y. Deng, L. Gong, A. Mi, X. Cui, Y. Jiang, M. C. Chio and A. S. Chan, *Tetrahedron: Asymmetry*, 2001, **12**, 1567–1571; (b) M. Nakoji, T. Kanayama, T. Okino and Y. Takemoto, *Org. Lett.*, 2001, **3**, 3329–3331; (c) M. Nakoji, T. Kanayama, T. Okino and Y. Takemoto, *J. Org. Chem.*, 2002, **67**, 7418–7423; (d) T. Kanayama, K. Yoshida, H. Miyabe, T. Kimachi and Y. Takemoto, *J. Org. Chem.*, 2003, **68**, 6197–6201; (e) T. Kanayama, K. Yoshida, H. Miyabe and Y. Takemoto, *Angew. Chem., Int. Ed.*, 2003, **42**, 2054–2056; (f) Y. Su, Y. Li, Y. Chen and Z. Han, *Chem. Commun.*, 2017, **53**, 1985–1988.
- 4 (a) K. Ohmatsu, N. Imagawa and T. Ooi, *Nat. Chem.*, 2014, **6**, 47–51; (b) K. Ohmatsu, S. Kawai, N. Imagawa and T. Ooi, *ACS Catal.*, 2014, **4**, 4304–4306.
- 5 M. Mechler and R. Peters, *Angew. Chem., Int. Ed.*, 2015, **54**, 10303–10307.
- 6 J. Schmid, T. Junge, J. Lang and R. Peters, *Angew. Chem., Int. Ed.*, 2019, **58**, 5447–5451.
- 7 (a) F. Willig, J. Lang, A. C. Hans, M. R. Ringenberg, D. Pfeffer, W. Frey and R. Peters, *J. Am. Chem. Soc.*, 2019, **141**, 12029–12043; (b) V. Miskov-Pajic, F. Willig, D. M. Wanner, W. Frey and R. Peters, *Angew. Chem., Int. Ed.*, 2020, **59**, 19873–19877.
- 8 R. C. D. Brown and J. F. Keily, *Angew. Chem., Int. Ed.*, 2001, **40**, 4496–4498.
- 9 R. A. Bhunnoo, Y. Hu, D. I. Laine and R. Brown, *Angew. Chem., Int. Ed.*, 2002, **41**, 3479–3480.
- 10 C. Wang, L. Zong and C.-H. Tan, *J. Am. Chem. Soc.*, 2015, **137**, 10677–10682.
- 11 (a) X. Ye, A. M. P. Moeljadi, K. F. Chin, H. Hirao, L. Zong and C.-H. Tan, *Angew. Chem., Int. Ed.*, 2016, **55**, 7101–7105; (b) K. F. Chin, X. Ye, Y. Li, R. Lee, A. M. Kabylda, D. Leow, X. Zhang, C. X. E. Ang and C.-H. Tan, *ACS Catal.*, 2020, **10**, 2684–2691.
- 12 L. Zong, C. Wang, A. M. P. Moeljadi, X. Ye, H. Hirao and C.-H. Tan, *Nat. Commun.*, 2016, **7**, 13455.
- 13 S. Paria, H. Lee and K. Maruoka, *ACS Catal.*, 2019, **9**, 2395–2399.
- 14 (a) H. J. Davis, M. T. Mihai and R. J. Phipps, *J. Am. Chem. Soc.*, 2016, **138**, 12759–12762; (b) H. J. Davis, G. R. Genov and R. J. Phipps, *Angew. Chem., Int. Ed.*, 2017, **56**, 13351–13355; (c) H. J. Davis, G. R. Genov and R. J. Phipps, *ACS Catal.*, 2018, **8**, 3764–3769.
- 15 G. R. Genov, J. L. Douthwaite, A. S. Lahdenpera, D. Gibson and R. J. Phipps, *Science*, 2020, **367**, 1246–1251.
- 16 H. Shi, A. N. Herron, Y. Shao, Q. Shao and J. Yu, *Nature*, 2018, **558**, 581–585.
- 17 (a) V. Cesar, N. Lughan and G. Lavigne, *J. Am. Chem. Soc.*, 2008, **130**, 11286–11287; (b) V. Cesar, N. Lughan and G. Lavigne, *Chem.-Eur. J.*, 2010, **16**, 11432–11442; (c) S. Kronig, E. Theuerberg, C. G. Daniliuc, P. G. Jones and M. Tamm, *Angew. Chem., Int. Ed.*, 2012, **51**, 3240–3244; (d) V. Cesar, C. Barthes, Y. Farre, S. Cuisiat, B. Y. Vacher, R. Brousses, N. Lughan and G. Lavigne, *Dalton Trans.*, 2013, **42**, 7373–7385.
- 18 A. Rabier, N. Lughan, R. Mathieu and G. L. Geoffroy, *Organometallics*, 1994, **13**, 4676–4678.
- 19 M.-J. Li, B. W.-K. Chu and V. W.-W. Yam, *Chem.-Eur. J.*, 2006, **12**, 3528–3537.
- 20 (a) M. Schroder, W. P. Griffith and J. C. S. Chem, *Comm*, 1979, 58–59; (b) G. Green, W. P. Griffith, D. M. Hollinshead, S. V. Ley and M. Schroder, *J. Chem. Soc., Perkin Trans. 1*, 1984, **15**, 681–686; (c) W. P. Griffith, S. V. Ley, G. P. Whitcombe, A. D. White and J. C. S. Chem, *Comm*, 1987, 1625–1627.
- 21 For selected reports of ferrate in oxidation see: (a) V. K. Sharma, J. T. Bloom and V. N. Joshi, *J. Environ. Sci. Health, Part A: Toxic/Hazard. Subst. Environ. Eng.*, 1998, **33**, 635–650; (b) V. K. Sharma, W. Rivera, V. N. Joshi, F. J. Millero and D. O'Connor, *Environ. Sci. Technol.*, 1999, **33**, 2545–2650; (c) M. Feng and V. K. Sharma, *Chem. Eng. J.*, 2018, **341**, 137–145; (d) C. Luo, M. Feng, V. K. Sharma and C.-H. Huang, *Environ. Sci. Technol.*, 2019, **53**, 5272–5281.
- 22 K. Manoli, G. Nakhla and A. K. Ray, *AIChE J.*, 2017, **63**, 4998–5006.
- 23 S. Li, B. Zhu, R. Lee, B. Qiao and Z. Jiang, *Org. Chem. Front.*, 2018, **5**, 380–385.

